Coupled defect-level recombination: Theory and application to anomalous diode characteristics

Andreas Schenk[a] and Ulrich Krumbein
Swiss Federal Institute of Technology, Integrated Systems Laboratory, Gloriastrasse 35, CH-8092 Zürich, Switzerland

(Received 13 March 1995; accepted for publication 11 May 1995)

We calculated the steady-state recombination rate for two coupled defect levels and implemented the model into a device simulator. This model generalizes the familiar single-level Shockley–Read–Hall (SRH) formula. If the intercenter transition probability vanishes, it reduces to the sum of two individual SRH rates, which are only linked via the band occupancies. The cases, where one of the levels or even both behave like traps in carrier capture, and the case of a rate-limiting intercenter transition are derived from the general expression. The important feature of the model is a possible increased field effect which might lead to large excess currents. The field effect is discussed in terms of tunnel-assisted multiphonon capture or direct tunneling into the levels, respectively. We show by means of numerical simulation that the large ideality factors found for liquid phase epitaxy grown diodes with weak intrinsic fields can be the result of a rapid direct charge transfer between donors and acceptors and the high probability of tunneling into the hydrogenic states. © *1995 American Institute of Physics.*

I. INTRODUCTION

Usually, recombination in semiconductors is well described by the Shockley–Read–Hall (SRH) model,[1,2] where electrons and holes are captured by a single defect level. Even if several levels are taken into account, they are considered as being independent from each other, apart from the indirect statistical link via the occupation in the bands. However, Chen *et al.*[3] found experimental evidence that intercenter charge transfer in silicon is efficient in trapping and recombination, beyond the framework of the single-level SRH model. They identified the shallow hydrogenic level of the P donor as an efficient recombination channel due to its coupling with the deep levels related to the vacancy-oxygen (V-O) complex. Rapid, direct charge transfer between two *deep* defects in silicon was reported by Frens *et al.*[4] They could show that the loosely bound electron of the interstitial carbon-interstitial oxygen ($C_i - O_i$) pseudodonor is lost to the V-O complex without the intermediate of the conduction band. This transfer process was found to be faster than 50 ns. Pseudodonors or pseudoacceptors strongly facilitate the interdefect mechanism due to their extended wave functions.

IV measurements of Liquid Phase Epitaxy (LPE) grown junctions in thin-film solar cells[5] revealed ideality factors of 3 and larger in the low forward-bias range. The maximum intrinsic field in these diodes does not support the assumption of defect-assisted tunneling via *midgap* levels. Also the large excess currents of *pin*-diodes grown by Molecular Beam Epitaxy (MBE) at low temperatures[6] can hardly be explained by this mechanism. Both types of thin-film devices seem to have a recombination channel which is much more sensitive to the field strength and which could be correlated to an interlevel transition.

In this paper we develop a model of coupled defect-level recombination and study the possible field enhancement. In Sec. II A the steady-state rate is derived as a generalization of the single-level SRH formula. The conditions for the efficiency of the mechanism will be outlined. The calculation of the field effect in Section II B is based on two different capture processes: field-enhanced multiphonon transitions and direct tunneling. Section III presents results of numerical simulations using the advanced device simulator DESSIS_ISE. The discussion in Section IV focusses on the effect of different two-level systems on the ideality of diode characteristics.

II. THEORY OF COUPLED DEFECT-LEVEL RECOMBINATION

A. Steady-state recombination rate

In Fig. 1 we illustrate all possible capture and emission processes for two coupled single-level recombination centers. Each level can exchange carriers with the conduction and valence band and with the other level. The deviation from SRH recombination via two independent levels is determined by the size of the interlevel capture and emission probabilities c_{12} and e_{12}, respectively. Such a process could be either a radiative intercenter transition between two defect states, a nonradiative cascade transition via a dense distribution of defect-levels, or a tunneling transition including a multiphonon decay as illustrated in Fig. 2. Here, we will not develop a microscopic theory for c_{12} and e_{12}, but use them as model parameters only.

The net rates for electrons and holes in the bands are (see Fig. 1)

$$R_n = N_{t1}[(1-f_{t1})c_{n1} - f_{t1}e_{n1}] + N_{t2}[(1-f_{t2})c_{n2} - f_{t2}e_{n2}], \tag{1}$$

$$R_p = N_{t1}[f_{t1}c_{p1} - (1-f_{t1})e_{p1}] + N_{t2}[f_{t2}c_{p2} - (1-f_{t2})e_{p2}], \tag{2}$$

where f_{t1} and f_{t2} denote the occupation probabilities and $c_{n1,2}$, $c_{p1,2}$, $e_{n1,2}$, $e_{p1,2}$ the capture and emission *probabili-*

[a]Electronic mail: schenk@iis.ee.ethz.ch

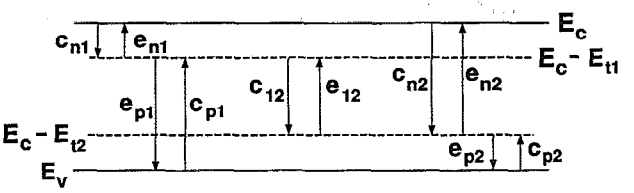

FIG. 1. Notation for all capture and emission processes via two coupled defect-levels.

ties per time for electrons and holes of levels 1 and 2, respectively. These latter quantities differ from the usual definitions of capture and emission coefficients with the dimension $cm^{-3}s^{-1}$. N_{t1} and N_{t2} are the defect densities. From Eqs. (1) and (2) the total steady-state recombination rate ($R_n=R_p=R$) can be written as

$$R=N_{t1}\frac{d_1}{d_2}(f_{t1}-\varphi_{t1})\,(c_{n2}+e_{n2})+N_{t1}[(1-f_{t1})c_{n1} -f_{t1}e_{n1}]+N_{t2}[(1-\varphi_{t2})c_{n2}-\varphi_{t2}e_{n2}] \tag{3}$$

with the abbreviation $d_{1,2}=c_{n1,2}+e_{n1,2}+c_{p1,2}+e_{p1,2}$. In deriving Eq. (3) f_{t2} has been expressed by f_{t1}, and $\varphi_{t1,2}$ labels the steady-state occupation probabilities of *noncoupled* defect-levels

$$\varphi_{t1,2}=\frac{1}{d_{1,2}}(c_{n1,2}+e_{p1,2}). \tag{4}$$

In the following the Greek symbol φ will be used for noncoupled levels. The occupation probability f_{t1} which determines the rate R according to Eq. (3) follows from the conditions of stationarity at level 1 and level 2:

$$(c_{n1}+e_{p1})+N_{t2}f_{t2}e_{12}=f_{t1}(d_1+N_{t2}c_{12}) +N_{t2}f_{t1}f_{t2}(e_{12}-c_{12}), \tag{5}$$

$$(c_{n2}+e_{p2})+N_{t1}f_{t1}c_{12}=f_{t2}(d_2+N_{t1}e_{12}) +N_{t1}f_{t1}f_{t2}(c_{12}-e_{12}). \tag{6}$$

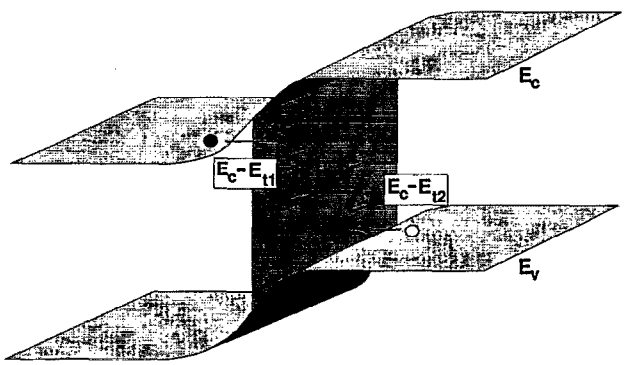

FIG. 2. Tunnel-assisted electron and hole capture into sublevels of the two defects. Recombination is completed by an intercenter transition accompanied by multiphonon emission. The defects are assumed to accumulate within the junction plane.

Solving that system for f_{t1} results in the following quadratic equation:

$$f_{t1}^2\,N_{t1}(c_{12}-e_{12})+f_{t1}\left[d_2+N_{t2}\frac{d_2}{d_1}\,c_{12}+N_{t1}e_{12} +\left(N_{t1}\varphi_{t1}+N_{t2}\frac{d_2}{d_1}\,\varphi_{t2}\right)(e_{12}-c_{12})\right]-d_2\varphi_{t1} -\left(N_{t1}\varphi_{t1}+N_{t2}\frac{d_2}{d_1}\,\varphi_{t2}\right)e_{12}=0. \tag{7}$$

The capture and emission probabilities $c_{n1,p2}$ and $e_{n1,p2}$ are defined in such a way that defect-assisted tunneling can be naturally incorporated by the field-dependent densities of states $N_{c,v}$ (Franz-Keldysh effect[7,8]):

$$\left.\begin{matrix}c_{n1}\\ e_{n1}\end{matrix}\right\}=\int_{E_c-E_{t1}}^{\infty}dE\;N_c(E)\times\left\{\begin{matrix}c_{n1}(E)f_c(E)\\ e_{n1}(E)[1-f_c(E)]\end{matrix}\right.,$$

$$\left.\begin{matrix}c_{p2}\\ e_{p2}\end{matrix}\right\}=\int_{-\infty}^{E_c-E_{t2}}dE\;N_v(E)\times\left\{\begin{matrix}c_{p2}(E)[1-f_v(E)]\\ e_{p2}(E)f_v(E)\end{matrix}\right. \tag{8}$$

(E—energy, $E_{t1,2}$—defect levels measured from the conduction band edge). In thermodynamic equilibrium detailed balance must hold between two arbitrary states of the energy spectrum to meet the requirement of microscopic reversibility. Thus, we can express the emission rates in terms of the capture rates

$$e_{n1}(E)=c_{n1}(E)\frac{(1-f_{t1}^0)f_0(E)}{f_{t1}^0[1-f_0(E)]} =c_{n1}(E)\frac{g_0^1}{g_1^1}\exp\left(\frac{E_c-E_{t1}-E}{k_BT}\right),$$

$$e_{p2}(E)=c_{p2}(E)\frac{f_{t2}^0[1-f_0(E)]}{f_0(E)(1-f_{t2}^0)} =c_{p2}(E)\frac{g_1^2}{g_0^2}\exp\left(-\frac{E_c-E_{t2}-E}{k_BT}\right) \tag{9}$$

($g_{0,1}^{1,2}$—degeneracy factors of the empty and occupied levels, respectively). Since in thermodynamic equilibrium detailed balance also holds between levels E_{t1} and E_{t2}, one obtains

$$e_{n1}=c_{n1}\frac{1-\varphi_{t1}^n}{\varphi_{t1}^n},\quad e_{p2}=c_{p2}\frac{\varphi_{t2}^p}{1-\varphi_{t2}^p},$$

$$e_{12}=c_{12}\frac{g_1^1g_0^2}{g_0^1g_1^2}\exp\left(-\frac{E_{t2}-E_{t1}}{k_BT}\right), \tag{10}$$

with $\varphi_{t1,2}^{n,p}$ being the occupation probabilities of the noncoupled defect-levels

$$\varphi_{t1,2}^{n,p}=\left[1+\frac{g_0^{1,2}}{g_1^{1,2}}\exp\left(\frac{E_c-E_{t1,2}-E_{Fn,p}}{k_BT}\right)\right]^{-1} \tag{11}$$

and $E_{Fn,p}$ the quasi Fermi energies of electrons and holes. Furthermore, electron and hole lifetimes for the non-coupled defects can be introduced:

$$\tau_{n1,2}=\frac{n}{N_{t1,2}\,c_{n1,2}}, \quad \tau_{p1,2}=\frac{p}{N_{t1,2}\,c_{p1,2}}. \tag{12}$$

Here, n and p denote the free electron and hole densities, respectively. The coupling parameter is most conveniently written as an internal rate (dimension $s^{-1}cm^{-3}$):

$$r_{12}=N_{t1}N_{t2}c_{12}. \tag{13}$$

Then, with the abbreviation

$$\epsilon=\frac{g_1^1 g_0^2}{g_0^1 g_1^2}\exp\left(-\frac{E_{t2}-E_{t1}}{k_BT}\right), \tag{14}$$

the quadratic equation for f_{t1} (7) takes the form

$$f_{t1}^2+f_{t1}\,(1-\xi_1)-\xi_1+\xi_2=0, \tag{15}$$

where

$$\xi_1=\frac{r_2}{r_{12}\tau_{n2}\tau_{p2}(1-\epsilon)}+\frac{1}{1-\epsilon}\left(1+\frac{r_2\tau_{n1}\tau_{p1}}{r_1\tau_{n2}\tau_{p2}}\right)-\left(\varphi_{t1}+\frac{r_2\tau_{n1}\tau_{p1}}{r_1\tau_{n2}\tau_{p2}}\,\varphi_{t2}\right), \tag{16}$$

$$\xi_2=\frac{r_2(1-\varphi_{t1})}{r_{12}\tau_{n2}\tau_{p2}(1-\epsilon)}+\frac{1}{1-\epsilon}\left[1-\varphi_{t1}+\frac{r_2\tau_{n1}\tau_{p1}}{r_1\tau_{n2}\tau_{p2}}(1-\varphi_{t2})\right], \tag{17}$$

$$\varphi_{t1,2}=\varphi_{t1,2}^n\left(1-\frac{\tau_{n1,2}}{n}\,R_{1,2}\right). \tag{18}$$

R_1, R_2 denote the net SRH recombination rates for the noncoupled defects[1] with the denominators abbreviated by r_1 and r_2:

$$R_{1,2}=\frac{np-n_i^2}{r_{1,2}}=\frac{np-n_i^2}{\tau_{n1,2}(p+p_{1,2})+\tau_{p1,2}(n+n_{1,2})}. \tag{19}$$

Equation (15) holds for Fermi statistics. In the following we will restrict ourselves to the nondegenerate case. With the definitions

$$n_{1,2}=n\,[(\varphi_{t1,2}^n)^{-1}-1]=N_c\frac{g_0^{1,2}}{g_1^{1,2}}\exp\left(-\frac{E_{t1,2}}{k_BT}\right), \tag{20}$$

$$p_{1,2}=p\,[(\varphi_{t1,2}^p)^{-1}-1]^{-1}=N_v\frac{g_1^{1,2}}{g_0^{1,2}}\exp\left(-\frac{E_g-E_{t1,2}}{k_BT}\right), \tag{21}$$

the total recombination rate (3) can be written as

$$R=R_1+R_2+\frac{n}{\tau_{n1}}\left(\frac{\frac{\tau_{n1}(p+p_1)}{\tau_{p1}(n+n_1)}\,\frac{\tau_{p2}(n+n_2)}{\tau_{n2}(p+p_2)}-1}{\frac{\tau_{p2}(n+n_2)}{\tau_{n2}(p+p_2)}+1}\right)\frac{f_{t1}-\varphi_{t1}}{\varphi_{t1}^n}. \tag{22}$$

Inserting the solution of the quadratic equation (15) for f_{t1}, using Eqs. (20), (21) and carrying out proper algebraic manipulations results in the following final form for R:

$$R=R_1+R_2+(\sqrt{R_{12}^2-S_{12}}-R_{12})\times\frac{\tau_{n1}\tau_{p2}(n+n_2)(p+p_1)-\tau_{n2}\tau_{p1}(n+n_1)(p+p_2)}{r_1\,r_2} \tag{23}$$

with

$$R_{12}=\frac{r_1\,r_2}{2r_{12}\tau_{n1}\tau_{n2}\tau_{p1}\tau_{p2}(1-\epsilon)}+\frac{1}{2\tau_{n1}\tau_{p2}(1-\epsilon)}\times[\tau_{n1}(p+p_1)+\tau_{p2}(n+n_2)]+\frac{\epsilon}{2\tau_{n2}\tau_{p1}(1-\epsilon)}[\tau_{n2}(p+p_2)+\tau_{p1}(n+n_1)], \tag{24}$$

$$S_{12}=\frac{1}{\tau_{n1}\tau_{p2}(1-\epsilon)}\left(1-\frac{\tau_{n1}\tau_{p2}}{\tau_{n2}\tau_{p1}}\,\epsilon\right)(np-n_i^2). \tag{25}$$

The coupled defect-level recombination rate (23) has the required symmetry with respect to a simultaneous exchange of index 1 with 2 and n with p. If the levels are decoupled ($r_{12}\to 0$), the total rate turns into the sum of the single-level recombination rates ($R\to R_1+R_2$). If both levels are identical, one obtains $R\to 2R_1(=2R_2)$. It is worthwhile to study the following special cases:

$\tau_{n2}\to\infty$.

No carrier exchange between the lower level and the conduction band. Such a system could be a midgap level coupled to a shallow acceptor-like level. In this case

$$R=R_1+\left(R_{12}-\sqrt{R_{12}^2-\frac{np-n_i^2}{\tau_{n1}\tau_{p2}(1-\epsilon)}}\right)\frac{\tau_{p1}(n+n_1)}{r_1} \tag{26}$$

with

$$R_{12}=\frac{(p+p_2)r_1}{2r_{12}\tau_{n1}\tau_{p1}\tau_{p2}(1-\epsilon)}+\frac{\tau_{n1}(p+p_1)+\tau_{p2}(n+n_2)}{2\tau_{n1}\tau_{p2}(1-\epsilon)}. \tag{27}$$

If the interlevel transition is not rate-limiting ($\tau_{12}\ll\tau_{n1},\tau_{p2}$), and if we assume that $\epsilon\ll 1$ and $p_1\approx n_1\approx n_i$, $n_2\ll n_i$, then we obtain in the limits of strong reverse and forward bias, respectively,

$$R\to\begin{cases}R_1\left(1+\dfrac{\tau_{p1}}{\sqrt{\tau_{n1}\tau_{p2}}}\right) & \text{for } np\ll n_i^2 \text{ and } \tau_{p2}\gg\tau_{n1}\\ R_1\left(1+\dfrac{\tau_{p1}}{\tau_{n1}}\right) & \text{for } np\ll n_i^2 \text{ and } \tau_{p2}\ll\tau_{n1}\end{cases}, \tag{28}$$

$$R\to\begin{cases}R_1\left(1+\dfrac{n\tau_{p1}}{p\tau_{n1}}\right) & \text{for } np\gg n_i^2 \text{ and } \dfrac{p}{n}>\dfrac{\tau_{p2}}{\tau_{n1}}\\ R_1\left(1+\dfrac{\tau_{p1}}{\tau_{p2}}\right) & \text{for } np\gg n_i^2 \text{ and } \dfrac{p}{n}<\dfrac{\tau_{p2}}{\tau_{n1}}\end{cases} \tag{29}$$

$\tau_{p1}\to\infty$.

No carrier exchange between the upper level and the valence band. Such a system could be a midgap level coupled to a shallow donor-like level as illustrated in Fig. 3. In this case

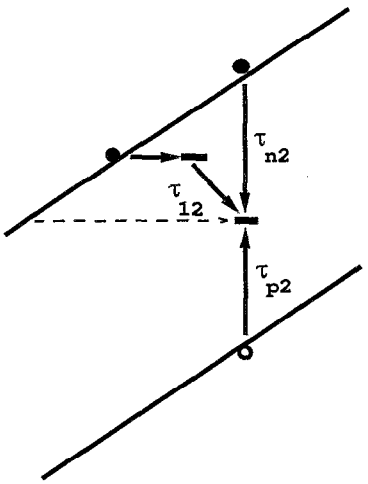

FIG. 3. Direct tunneling into the shallow donor-like state as a possible source of excess current. Tunneling into the midgap level is negligible because of the huge potential barrier. If $\tau_{12} \ll \tau_{n2}$, recombination via the upper level can become dominant, depending on its binding energy.

$$R = R_2 + \left(R_{12} - \sqrt{R_{12}^2 - \frac{np - n_i^2}{\tau_{n1}\tau_{p2}(1-\epsilon)}} \right) \frac{\tau_{n2}(p+p_2)}{r_2} \tag{30}$$

with

$$R_{12} = \frac{(n+n_1)r_2}{2r_{12}\tau_{n1}\tau_{n2}\tau_{p2}(1-\epsilon)} + \frac{\tau_{n1}(p+p_1)+\tau_{p2}(n+n_2)}{2\tau_{n1}\tau_{p2}(1-\epsilon)}. \tag{31}$$

If the interlevel transition is not rate-limiting ($\tau_{12} \ll \tau_{n1}, \tau_{p2}$), and if we assume that $\epsilon \ll 1$ and $n_2 \approx p_2 \approx n_i$, $p_1 \ll n_i$, then in the limits of strong reverse and forward bias, respectively,

$$R \to \begin{cases} R_1 \left(1 + \dfrac{\tau_{n2}}{\sqrt{\tau_{n1}\tau_{p2}}} \right) & \text{for } np \ll n_i^2 \text{ and } \tau_{n1} \gg \tau_{p2} \\ R_1 \left(1 + \dfrac{\tau_{n2}}{\tau_{p2}} \right) & \text{for } np \ll n_i^2 \text{ and } \tau_{n1} \ll \tau_{p2} \end{cases}, \tag{32}$$

$$R \to \begin{cases} R_2 \left(1 + \dfrac{\tau_{n2}}{\tau_{n1}} \right) & \text{for } np \gg n_i^2 \text{ and } \dfrac{p}{n} > \dfrac{\tau_{p2}}{\tau_{n1}} \\ R_2 \left(1 + \dfrac{p\tau_{n2}}{n\tau_{p2}} \right) & \text{for } np \gg n_i^2 \text{ and } \dfrac{p}{n} < \dfrac{\tau_{p2}}{\tau_{n1}} \end{cases} \tag{33}$$

$\tau_{n2} \to \infty$ and $\tau_{p1} \to \infty$.

In this case

$$R = R_{12} - \sqrt{R_{12}^2 - \frac{np - n_i^2}{\tau_{n1}\tau_{p2}(1-\epsilon)}} \tag{34}$$

with

$$R_{12} = \frac{(n+n_1)(p+p_2)}{2r_{12}\tau_{n1}\tau_{p2}(1-\epsilon)} + \frac{\tau_{n1}(p+p_1)+\tau_{p2}(n+n_2)}{2\tau_{n1}\tau_{p2}(1-\epsilon)}. \tag{35}$$

Let us assume now that the interlevel transition is *rate-limiting* ($\tau_{12} \gg \tau_{n1}, \tau_{p2}$). From Eq. (34) one obtains

$$R \to r_{12} \frac{np - n_i^2}{(n+n_1)(p+p_2)} \to \begin{cases} -r_{12} & \text{for } np \ll n_i^2 \\ r_{12} & \text{for } np \gg n_i^2 \end{cases}. \tag{36}$$

The condition for r_{12} becoming rate-limiting follows from Eq. (35):

$$r_{12} \ll \frac{(n+n_1)(p+p_2)}{2\sqrt{|np - n_i^2|}\sqrt{\tau_{n1}\tau_{p2}}\sqrt{1-\epsilon}}. \tag{37}$$

With $\epsilon \ll 1$ this gives in the limits of strong reverse and forward bias, respectively,

$$r_{12} \ll \begin{cases} \dfrac{n_i}{2\epsilon\sqrt{\tau_{n1}\tau_{p2}}} & \text{for } np \ll n_i^2 \\ \dfrac{\sqrt{n_p p_p}}{2\sqrt{\tau_{n1}\tau_{p2}}} \dfrac{n_1}{n_p}, \dfrac{\sqrt{n_n p_n}}{2\sqrt{\tau_{n1}\tau_{p2}}} \dfrac{p_2}{p_n} & \text{for } np \gg n_i^2 \end{cases}, \tag{38}$$

where n_p, p_n denote the minority carrier densities and n_n, p_p the majority carrier densities, respectively. Relation (38) is essential for the understanding of the efficiency of the coupled defect-level recombination process. It turns out that r_{12} becomes the bottleneck for recombination, if it is smaller than the product of a "combined trapping rate" (i.e., $n_i/\sqrt{\tau_{n1}\tau_{p2}}$ at reverse bias) and another limiting factor ($1/\epsilon$ at reverse bias, n_1/n_p or p_2/p_n at forward bias) which strongly depend on the position of the defect-levels in the gap and their energetic separation. These factors increase with decreasing distance of the levels to the band edges. As an example, using $n_i = 10^{10}$ cm^{-3}, $\tau_{n1} = \tau_{p2} = 10^{-5}$ s, and $E_{t1} = E_g - E_{t2} = 0.1$ eV yields $r_{12} \ll 10^{30}$ cm^{-3}s^{-1}, i.e., r_{12} becomes rate-limiting even for already extremely large interlevel transition rates and hence will drop the total recombination rate to a low value. Thus, in order to be able to compete with midgap single-level SRH recombination, the interlevel transition must either be very rapid or the energetic separation must not be too large. Therefore, a possible candidate for an efficient two-level system could involve a deep midgap level. The transition between P donor and (V-O) complex and the transition between ($C_i - O_i$) pseudodonor and (V-O) complex found in Refs. 3,4 are examples for such a scenario.

B. Field-enhancement of the recombination rate

It is well known[9,10] that defect-assisted tunneling can become a cause of "excess current" in diodes, if the electric field is sufficiently high. Simulations of Esaki diodes show that fields as high as 5×10^5 V/cm induce excess currents by field-assisted recombination via *midgap* centers.[11] However, deviations of forward-bias IV characteristics similar to those observed in the "excess current" range of Esaki diodes were also found in diodes having much lower peak fields. LPE-grown junctions with measured doping profiles that can pro-

duce fields of at most 1×10^5 V/cm in the low forward-bias range exhibited ideality factors of 3 and larger in this range.[5] The question arises if these anomalous IV curves can originate from field-enhanced recombination via a two-level system, where the tunnel barrier is considerably lower when at least one level is "shallow," or if charging effects in the junction plane (e.g., at grain boundaries) yield high local electric fields. One suitable test system to study this problem is a midgap recombination level coupled to a "shallow" donor-like level as described above. If the interlevel transition is not rate-limiting, the factor $(1+\tau_{n2}/\tau_{n1})$ in Eq. (33) could yield the field enhancement provided $\tau_{n1}\ll\tau_{n2}$ holds under realistic conditions. For the quantitative discussion of the field effect we must know the field dependence of the capture rate $c_{n1}(E)$ in Eq. (8) which determines the lifetime τ_{n1}. We will assume that the recombination process is a field-enhanced multiphonon decay,[12] and we will distinguish the cases of strong and zero electron-phonon coupling, respectively. The capture rate $c_{n1}(E)$ then takes the form

$$c_{n1}(E)=\frac{(4\pi)^2 r_{t1}^3}{\hbar}\,e^{-S_1(2f_B+1)}\sum_{l=-\infty}^{\infty}\left[r_F^2+\frac{(S_1-l)^2}{S_1}\,r_{ph}^2\right]\times\left(\frac{f_B+1}{f_B}\right)^{l/2} I_l(2S_1\sqrt{f_B(f_B+1)})\;\delta(l\hbar\omega_1+E_c-E_{t1}-E). \tag{39}$$

The symbols in Eq. (39) have the following meaning: I_l—modified Bessel function of order l, S_1—Huang–Rhys factor (a measure of the coupling strength of the diagonal electron–phonon coupling of defect level 1), $f_B=[\exp(\hbar\omega_1/k_BT)-1]^{-1}$—Bose function, $\hbar\omega_1$—effective phonon energy for the phonon coupling of defect level 1, r_{t1}—localization radius of the defect state 1. The assumption of a single representative phonon mode reduces the integral in Eq. (8) to a sum over discrete energies separated by $\hbar\omega_1$. A 3D Dirac potential has been used for the defect to obtain the prefactor in Eq. (39). The matrix elements of electron-field and electron–phonon coupling, r_F^2 and r_{ph}^2, are modeled in the following way:

$$r_F^2=q^2F^2|x_{c,t1}|^2, \tag{40}$$

$$r_{ph}^2=\frac{D_{opt}^2\hbar}{\rho\omega_1 a^3}\,q_0^2|x_{c,t1}|^2, \tag{41}$$

where deformation potential coupling to optical phonons has been assumed. Therefore, $\hbar\omega_1$ is the energy of an optical phonon and q_0 its wave number. D_{opt} denotes the deformation potential constant, $F=F(\mathbf{x})$ the electric field at position x, ρ the mass density, and a the lattice constant. The transition matrix element $x_{c,t1}$ of the position operator can only be estimated; we use $|x_{c,t1}|^2\approx\hbar^2/(2E_{t1}m_c)$ with the conduction band effective mass m_c which will also be used for the tunneling mass.

Assuming parabolic and isotropic bands, the field-dependent density of states in the conduction band is given by

$$N_c(E,F)=\frac{1}{2\pi}\left(\frac{2m_c}{\hbar^2}\right)^{3/2}\sqrt{\hbar\Theta_c(F)}\;\mathcal{F}\left[\frac{E_c(x)-E}{\hbar\Theta_c(F)}\right], \tag{42}$$

with $\mathcal{F}(y)=Ai'^2(y)-y\,Ai^2(y)$, $y=(E_c(x)-E)/\hbar\Theta_c(F)$, and $\Theta_c(F)=(q^2F^2/2\hbar m_c)^{1/3}$. Equation (42) describes the tunnel probability across a triangular barrier. If the center is attractive prior to capture, the lowering of the potential barrier can be modeled by the 1D Poole–Frenkel effect.[13]

1. Strong electron-phonon coupling (high-temperature approximation)

In this case the capture rate $c_{n1}(E)$ Eq. (39) can be written in Gaussian form[14]

$$c_{n1}(E)=\frac{(4\pi)^2 r_{t1}^3 S_1 r_{ph}^2}{\hbar\sqrt{4\pi S_1\hbar\omega_1 k_BT}}\,e^{\frac{S_1\hbar\omega_1}{k_BT}}\times\exp\left[-\frac{(E-E_c+E_{t1}-S_1\hbar\omega_1)^2}{4S_1\hbar\omega_1 k_BT}\right], \tag{43}$$

and the lifetime given by Eq. (12) can be computed approximately. Inserting Eqs. (43) and (42) into Eq. (8) yields for the reciprocal lifetime

$$\tau_{n1}^{-1}(F)=\frac{4r_{t1}^3 N_{t1} S_1 r_{ph}^2\sqrt{\hbar\Theta_c(F)}}{\sqrt{\pi}\hbar(k_BT)^{3/2}(1+\sqrt{E_F/(E_{t1}-E_0)})^{1/2}}\times\exp\left(\frac{E_{t1}-E_0}{k_BT}\right)\mathcal{F}\left(\frac{E_{t1}-E_0}{\hbar\Theta_c(F)}\right)\times\exp\left[-\frac{E_{act}(F)}{k_BT}\right], \tag{44}$$

where E_0 denotes a field- and temperature-dependent transition energy measured from the level E_c-E_{t1} in direction to the conduction band, and $E_{act}(F)$ is a field-dependent activation energy for electron capture:

$$E_{act}(F)=\frac{(E_0-S_1\hbar\omega_1)^2}{4S_1\hbar\omega_1}, \tag{45}$$

$$E_0=2\sqrt{E_F}[\sqrt{E_F+E_{t1}+S_1\hbar\omega_1}-\sqrt{E_F}]-S_1\hbar\omega_1, \tag{46}$$

$$E_F=\frac{(2S_1\hbar\omega_1 k_BT)^2}{[\hbar\Theta_c(F)]^3}. \tag{47}$$

$E_{t1}-E_0$ equals the effective barrier height of the tunnel barrier, which approaches zero for vanishing electric field. The prefactor in Eq. (44) can be expressed by the zero-field reciprocal lifetime

$$\tau_{n1}^{-1}(0)=\frac{4r_{t1}^3 N_{t1} S_1 r_{ph}^2}{\pi^{3/2}\hbar\sqrt{k_BT}}\,\frac{S_1\hbar\omega_1}{(E_{t1}+S_1\hbar\omega_1)^{3/2}}\times\exp\left[-\frac{(E_{t1}-S_1\hbar\omega_1)^2}{4S_1\hbar\omega_1 k_BT}\right]. \tag{48}$$

2. Direct tunneling

If the electrons tunnel directly into state 1, the lifetime τ_{n1} turns into a macroscopic tunnel time constant. Without phonon participation the result for $c_{n1}(E)$ is

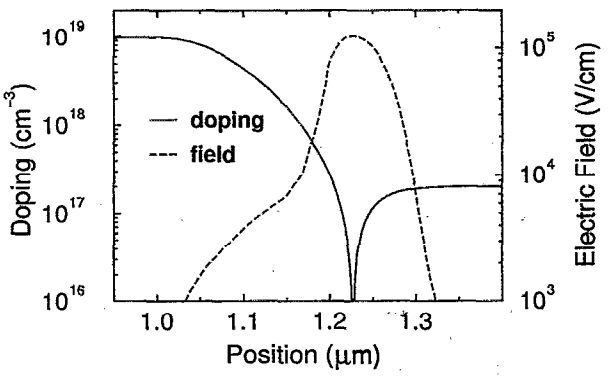

FIG. 4. Net doping profile and electric field distribution of the n^+p-junction used in the device simulation.

$$c_{n1}(E)=\frac{(4\pi)^2 r_{t1}^3}{\hbar}\, r_F^2\, \delta(E_c-E_{t1}-E), \tag{49}$$

and with Eq. (40) the reciprocal lifetime becomes

$$\tau_{n1}^{-1}(F)=\frac{4N_{t1}r_{t1}^3}{\sqrt{\pi}\hbar(k_BT)^{3/2}E_{t1}}[\hbar\Theta_c(F)]^{7/2} \times\exp\left(\frac{E_{t1}}{k_BT}\right)\mathscr{F}\left[\frac{E_{t1}}{\hbar\Theta_c(F)}\right]. \tag{50}$$

The unknown parameter in this expression is the fraction of defect volume $N_{t1}r_{t1}^3$.

III. SIMULATION RESULTS

The recombination model was implemented into the device simulator DESSIS$_{-\mathrm{ISE}}$ [15] in its general form [Eq. (23)]. Field-enhanced capture and emission can be taken into account for both defect levels, either in form of field-enhanced multiphonon transitions (44) (strong coupling) or in form of direct tunneling (50) (no coupling). The doping profile and intrinsic field of the simulated diode are shown in Fig. 4. The profile is based on spreading resistance measurements at LPE-grown p^+n-junctions of silicon thin-film solar cells produced at the University of New South Wales (UNSW), Kensington, Australia.[16] The metal solutions in the growing process were based on indium (In) and tin (Sn), respectively.[17] Note that the intrinsic electric field does not exceed 1.25×10^5 V/cm. The simulated forward-bias $j(V)$- and $n(V)$-characteristics are presented in comparison to the "type 1" data of Ref. 5. The $n(V)$-curves were calculated according to $n(V)=[U_T d(\ln j)/dV]^{-1}$ (U_T – thermal voltage). A finite shunt resistance was included in the simulation, but it only influences the characteristics up to 150 mV.

In Fig. 5 the results of three different scenarios are shown. The open circles define the ideal reference curve, where single-level SRH recombination via a midgap center ($E_t=E_i$) was assumed. Defect-assisted tunneling has no effect due to the low field strength. The solid line results, if this level is coupled with the indium level ($E_{t2}=E_v+0.157$ eV). The value of the interlevel transition rate was chosen such that it did not limit the total rate. Despite the assumed strong electron-phonon coupling, tunneling is not enhanced to a level necessary for a visible excess current. Therefore, this case gives the same characteristic as single-level SRH recombination. In the third scenario the midgap center was coupled to a shallow donor (As, $E_{t1}=E_c-0.054$ eV), again assuming that the interlevel rate is not limiting. Now, the tunnel barrier is sufficiently small for direct tunneling to yield a large excess current. The shape of the n-peak becomes similar to the measured one. Assuming a shallow acceptor instead of the donor yields qualitatively equal results. The excess current can be increased by: increasing the fraction of defect volume, lowering the binding energy of the shallow level, or reducing the lifetimes of the midgap level. However, it is impossible to obtain a maximum of $n(V)$ larger than 3 and, at the same time, a shape of the n-peak which is similar to the measured one.

Figure 6 shows the simulation results, if one assumes that the coupled defect-level mechanism is a donor-acceptor pair recombination in conjunction with direct tunneling into both shallow levels. The rate r_{12} of the pair recombination itself was set to infinity in order to avoid any effect on the total rate. A parallel single-level SRH process via a midgap

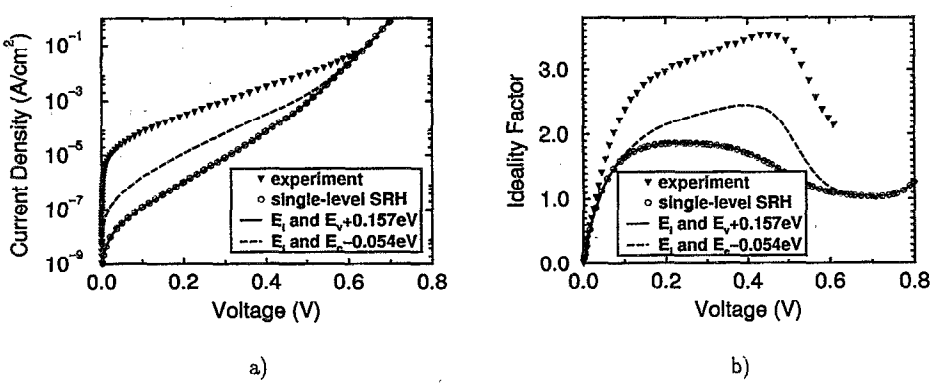

FIG. 5. (a) Simulated and measured $j(V)$-characteristics of the diode characterized in Fig. 4. Solid curve: multiphonon coupling, $E_{t1}=E_i$, $E_{t2}=E_v+0.157$ eV, $r_{12}=10^{29}$ cm^{-3}s^{-1}, $\tau_{n1}=10^{-7}$ s, $\tau_{p1}=10^{-8}$ s, $\tau_{n2}=\infty$, $\tau_{p2}=10^{-7}$ s; dashed curve: direct tunneling, $E_{t1}=E_c-0.054$ eV, $E_{t2}=E_i$, $r_{12}=10^{27}$ cm^{-3}s^{-1}, τ_{n1}—determined by direct tunneling, $\tau_{p1}=\infty$, $\tau_{n2}=10^{-7}$ s, $\tau_{p2}=10^{-8}$ s, fraction of defect volume $=10^{-2}$; open circles: single-level SRH recombination with $E_t=E_i$, $\tau_n=10^{-7}$ s, $\tau_p=10^{-8}$ s. (b) Corresponding $n(V)$-characteristics.

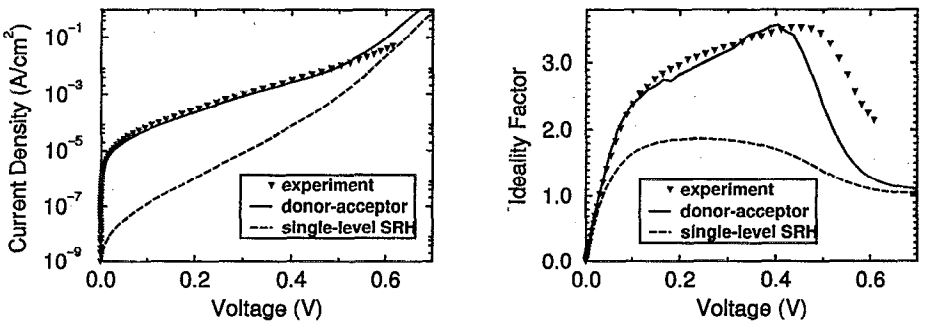

FIG. 6. (a) Simulated and measured $j(V)$-characteristics of the diode characterized in Fig. 4. Solid curve: donor-acceptor pair recombination with direct tunneling and parallel single-level SRH recombination, $E_{t1}=E_c-0.045$ eV, $E_{t2}=E_v+0.045$ eV, $r_{12}=\infty$, τ_{n1}—determined by direct tunneling, $\tau_{p1}=\infty$, $\tau_{n2}=\infty$, τ_{p2}—determined by direct tunneling, fraction of defect volume = 0.04, single-level parameters: $E_t=E_i$, $\tau_n=10^{-8}$ s, $\tau_p=10^{-9}$ s; dashed curve: only single-level SRH recombination with $E_t=E_i$, $\tau_n=10^{-7}$ s, $\tau_p=10^{-8}$ s. (b) Corresponding $n(V)$-characteristics.

level was allowed. Hole tunneling increases the field effect to the observed large excess current in the low-voltage range. Barrier lowering was not taken into account, but decreasing the binding energies and reducing the fraction of defect volume to keep the tunnel times equal, yields similar results.

IV. DISCUSSION

The coupled defect-level recombination process with a rapid and not rate-limiting interlevel transition is a possible cause of the large excess currents observed in the $j(V)$-characteristics of LPE-grown diodes with moderate intrinsic fields. If the large ideality factors are to be explained by a field effect, single-level SRH recombination can be ruled out. A field of not more than 1.25×10^5 V/cm as supposed to be present in the discussed pn-junctions, can not visibly enhance the forward-bias SRH current. For an increase of the current by three orders of magnitude one would need about 6×10^5 V/cm. Applying the two-level model and shifting one level to a band edge for a sufficient tunnel probability, but still assuming that the mechanism for the transition into that level remains multiphonon recombination, does not yield a large enough field effect as well (see Fig. 5). The reason for this behavior is that at room temperature the effective thermal probability of the transition can not be enhanced by three orders, not because of the weak field, but because the thermal probability itself does not increase by three orders over the energy interval which is gained by the action of the field. This is in contrast to strongly localized midgap centers, where the thermal probability of capture and emission can vary over 20 or 30 orders within $E_g/2$, and therefore, the tunnel effect can enhance the recombination current drastically.

If a shallow level belongs to the two-level system, carriers can also tunnel directly into the state. Then, the possible field effect is within the variation of the tunnel time constants as function of the field strength. This strong variation is correlated to the growing width of the tunnel barriers as the forward-bias increases. As a consequence: if the large current in the low-voltage range is the result of tunneling, then the shape of the n-peak is sensitive to the details of the potential. Thus, it is hardly possible to get a close fit. Moreover, the tunneling transition can involve phonons, e.g. one-phonon scatterings. The test system consisting of a midgap recombination center and a shallow donor (acceptor) yields a considerable excess current, if the interlevel transition is assumed not to limit the rate. The measured shape of the n-peak can also be reproduced, but both the current density and the height of the n-peak remain still too small (see Fig. 5). Decreasing the tunneling time by changing the depth of the shallow level or the amount of defects can further increase the excess current, but not the size of the ideality factor.

In order to obtain a larger n it was found that the field effect must become even stronger. As another system we considered a (infinitely fast) donor-acceptor pair recombination with direct tunneling into the shallow levels, together with a parallel single-level SRH recombination channel which is always present in the device. This mechanism gives the large excess currents observed for low voltages and the right slope up to 400 mV. The shape of the n-peak is mainly determined by the transition from recombination current to diffusion current, where in the case of an ideal diode the ideality factor changes from 2 to 1 (compare Fig. 5(b)). The recombination-dominated range is covered by the excess current, which starts to disappear in the measurement not before 500 mV. For this voltage the field maximum is about 6×10^4 V/cm only. This value is insufficient for significant tunneling into levels of 45 mV binding energy assuming a triangular barrier, hence the excess current mechanism "switches off" earlier in the simulation. Due to the thin-film fabrication process there is a high probability for the formation of pairs of donors (phosphorus) and acceptors (aluminium) at the metallurgical junction. These pairs could accumulate with a high concentration in a very thin layer. The low rate measured by EPR in Ref. 18 was found for specimens with a random distribution of phosphorus and boron and doping levels of the order of 10^{16} cm^{-3}. Moreover, the recombination rate strongly increased with rising doping and temperature. The resulting tunnel barrier of those donor-acceptor pairs which is seen by the carriers, is hard to determine. Therefore, we used triangular barriers neglecting the

dipole character of the pairs and also skipped the (unknown) Poole-Frenkel barrier lowering.

Low-temperature photoluminescence spectra[19] indicated a strong donor-acceptor pair recombination between the P donor and the In acceptor in In-doped silicon LPE-layers grown with a small cooling rate. The Poole-Frenkel effect is significant for the metal impurities Sn ($E_c - 0.25$ eV) and In ($E_v + 0.157$ eV) making direct tunneling a very probable process. We found that large ideality factors can occur, if these levels are assumed to couple to the shallow levels. However, there is no combination that nearly gave the measured size of the excess current in the low forward-bias range.

ACKNOWLEDGMENTS

The authors are grateful to S. Robinson from the University of New South Wales (UNSW), Kensington for providing the experimental data and for many stimulating discussions. He also outlined the idea of intercenter recombination as a possible source for the anomalous $j(V)$-characteristics.

[1] W. Shockley and W. T. Read, Phys. Rev. **87**, 835 (1952).
[2] R. N. Hall, Phys. Rev. **87**, 387 (1952).
[3] W. M. Chen, B. Monemar, E. Janzen, and J. L. Lindström, Phys. Rev. Lett. **67**, 1914 (1991).
[4] A. M. Frens, M. T. Bennebroek, A. Zakrzewski, J. Schmidt, W. M. Chen, E. Janzen, J. L. Lindström, and B. Monemar, Phys. Rev. Lett. **72**, 2939 (1994).
[5] S. J. Robinson, G. F. Zheng, W. Zhang, Z. Shi, and M. A. Green, in Extended Abstracts of the 12th EC PVSEC, Amsterdam, Netherlands, 1994.
[6] H. Jorke, H. Kibbel, K. Strohm, and E. Kasper, Appl. Phys. Lett. **63** (1993).
[7] W. Franz, Z. Naturforsch. **13a**, 484 (1958).
[8] L. V. Keldysh, Sov. Phys. JETP **6**, 763 (1958).
[9] A. G. Chynoweth and R. A. Logan, Proc. Int. Conf. Phys. Sem., Prague, Czech. J. Phys., special publication, pages 201–203, 1960.
[10] A. G. Chynoweth, W. L. Feldmann, and R. A. Logan, Phys. Rev. **121**, 684 (1961).
[11] A. Schenk, U. Krumbein, S. Müller, H. Dettmer, and W. Fichtner, IEICE Trans. Electron. (Japan) **E77-C**, 148 (1994).
[12] A. Schenk, J. Appl. Phys. **71**, 3339 (1992).
[13] J. Frenkel, Phys. Rev. **54**, 647 (1938).
[14] A. Schenk, Solid-State Electron. **35**, 1585 (1992).
[15] S. Müller, K. Kells, A. Benvenuti, J. Litsios, U. Krumbein, A. Schenk, and W. Fichtner, DESSIS 1.3.6: Manual. Technical report, ISE Integrated Systems Engineering AG, 1994.
[16] S. Robinson, University of New South Wales, Kensington, Australia (private communication).
[17] R. Bergmann, S. Robinson, Z. Shi, and J. Kurianski, Solar Energy Mat. Solar Cells **31**, 447 (1993).
[18] V. S. Vavilov, O. G. Koshelev, Yu. P. Koval', and Ya. G. Klyava, Sov. Phys. Solid State **8**, 2770 (1967).
[19] W. Schmid, U. Nieper, and J. Weber, Solid State Commun. **45**, 1007 (1983).